SUPPLMENTAL MATERIAL

Table S1. Information of Healthy donors and CHD-PAH patients providing serum for this project.

Healthy donor

NO.	Sex	Age
1	male	9 months
2	male	1 years
3	male	3 years
4	female	1 years
5	male	28 days
6	female	1 years
7	male	2 years
8	male	2 years
9	male	3 months + 23 days
10	female	3 years
11	male	16 hours
12	female	5 months + 9 days
13	male	3 months＋23days

CHD-PAH patients

NO.	Patient's ID	Sex	Age	Diagnosis
1	754937	female	1 years + 2 months	ASD, Mild PAH
2	757064	female	11 months	ASD, Mild PAH
3	757808	male	2 years + 6 months	ASD, Mild PAH
4	757833	female	1 years + 3 months	ASD, Moderate PAH
5	758474	male	4 years + 7 months	ASD, Severe PAH
6	759373	female	9 months	VSD, Mild PAH
7	761435	female	7 months	VSD, Mild PAH
8	771706	male	3 years + 1 months	VSD, Severe PAH
9	785003	male	5 months	ASD, Mild PAH
10	789888	female	5 months	VSD, Mild PAH
11	796058	male	2 years + 9 months	ASD, Mild PAH
12	797743	male	1 years	ASD, Mild PAH
13	799233	female	4 months	VSD, Severe PAH
14	804178	male	3 months	ASD, Mild PAH
15	804421	male	1 years + 7 months	ASD, Mild PAH
16	804626	female	3 years	ASD, Severe PAH
17	804694	female	6 months	VSD, Moderate PAH
18	805218	female	1 years	VSD, Severe PAH
19	805718	female	9 months	VSD, Moderate PAH
20	805926	male	4 years + 6 months	VSD, Severe PAH
21	805929	male	1 years + 3 months	VSD, Mild PAH
22	806394	male	6 months	ASD, Severe PAH
23	808020	female	9 months	ASD, Mild PAH
24	808091	male	6 months	ASD, Severe PAH
25	810394	male	1 years	ASD, Moderate PAH
26	811536	male	9 months	VSD, Severe PAH
27	811589	female	11 months	VSD, Mild PAH
28	812097	female	6 months	VSD, Mild PAH
29	813105	male	5 months	VSD, Severe PAH

Table S2. List of primers for vector construction, mRNA/ miRNA retro-transcription and qRT-PCR.

Name	Sequence (5'-3')	Purpose
rat-shHDAC4-P1	ACCGTGATATGTTCATGCAGCTGTGCTCGAGCAC AGCTGCATGAACATATCA	Construction of shHDAC4 vector
rat-shHDAC4-P2	AAAATGATATGTTCATGCAGCTGTGCTCGAGCAC AGCTGCATGAACATATCA	
rat-shDNMT1-P1	ACCGTATTGGTGCATACTCTGGGCTCTCGAGAGC CCAGAGTATGCACCAATA	Construction of shDNMT1 vector
rat-shDNMT1-P2	AAAATATTGGTGCATACTCTGGGCTCTCGAGAGC CCAGAGTATGCACCAATA	
rat-shEP300-P1	ACCGGCCAGTCCTATGGGTGTAAATCTCGAGATT TACACCCATAGGACTGGC	Construction of shEP300 vector
rat-shEP300-P2	AAAAGCCAGTCCTATGGGTGTAAATCTCGAGAT TTACACCCATAGGACTGGC	
hsa-HDAC4-3'UTR-F	CGGAATTCATCTCCTTCCACGGGCCAGGCGAG	Construction of HDAC4-3'UTR vector
hsa-HDAC4-3'UTR-R	CCGCTCGAGGGAGGGCAAGTAACGCAGTCTTTA	
hsa-PTPRD-3'UTR-F	CGGAATTCGACTGATGAGGCATCTGAAGGA	Construction of PTPRD-3'UTR vector
hsa-PTPRD-3'UTR-R	CCGCTCGAGTGATGTGCATTCCTCATTTCCC	
hsa-WNT3A-3'UTR-F	CGGAATTCCCCTGGGTGGAGCAGGACTC	Construction of WNT3A-3'UTR vector
hsa-WNT3A-3'UTR-R	CCGCTCGAGCAGCCTACCCCAGAGCCGTG	
hsa-HDAC4-3'UTR-mut-F	GTGTGTGCTCCATAGTCCTCCGCCTATTTTCCAAT TGATGAGAATG	Site-directed mutation of HDAC4-3'UTR vector
hsa-HDAC4-3'UTR-mut-R	CATTCTCATCAATTGGAAAATAGGCGGAGGACT ATGGAGCACACAC	
hsa-PTPRD-3'UTR-mut-F	CAACAGCCTCCGCCAAAGTATAAAGTTGCTGCTA ACATATATACATATAT	Site-directed mutation of PTPRD-3'UTR vector
hsa-PTPRD-3'UTR-mut-R	ACTTTGGCGGAGGCTGTTGATTCCAAAAACAAA ACAAAATAATAATTATC	
β-ACTIN-mRNA-F	AAAGACCTGTACGCCAACAC	qRT-PCR analysis of ACTIN mRNA level (reference control)
β-ACTIN-mRNA-R	GTCATACTCCTGCTTGCTGAT	
rat-HDAC4-mRNA-F	ACTCCTCTATGGCACAAACCC	qRT-PCR analysis of HDAC4 mRNA level
rat-HDAC4-mRNA-R	GCAAAGCCATTCTTTAGCTCT	
rat-PTPRD-mRNA-F	CGGTGTTGGAAGAACTGGAGTC	qRT-PCR analysis of PTPRD mRNA level
rat-PTPRD-mRNA-R	TGCATAGTGATCAAAGCTGCCC	
rat-KLF4-mRNA-F	GAAGGTCTTGGCCCCGGAAAAGAAC	qRT-PCR analysis of KLF4 mRNA level
rat-KLF4-mRNA-R	GGTAGTGCCTGGTCAGTTCATC	
rat-Klf2-mRNA-F	TGGAGCTGTTGGAGGCCAAGCC	qRT-PCR analysis of KLF2 mRNA level
rat-Klf2-mRNA-R	CTTGCGGTAGTGGCGGGTAAGC	
rat-SMAD3-mRNA-F	ACCAGGGCTTTGAGGCTGTCTA	qRT-PCR analysis of SMAD3 mRNA level
rat-SMAD3-mRNA-R	GTGAGGACCTTGTCAAGCCACT	
rat-CHOP-mRNA-F	CTCTGCCTTTCGCCTTTGAGAC	qRT-PCR analysis of CHOP mRNA level
rat-CHOP-mRNA-R	AGGGCTTTGGGAGGTGCTTGTG	
rat-TRIB3-mRNA-F	TTTCCGACAGATGGCTAGTGCG	qRT-PCR analysis of TRIB3 mRNA level
rat-TRIB3-mRNA-R	GATGGCCGGGAGCTGAGTATCT	
rat-VEGF-mRNA-F	ACTGTGAGCCTTGTTCAGAGCG	qRT-PCR analysis of VEGF mRNA level
rat-VEGF-mRNA-R	GACATGGTTAATCGGTCTTTCC	
rat-GLUT1-mRNA-F	ATGGTTCATTGTGGCCGAGCTG	qRT-PCR analysis of GLUT1 mRNA level
rat-GLUT1-mRNA-R	CCGGCCTTTGGTCTCAGGAACT	
rat-HIF-1α-mRNA-F	ACTATGTCGCTTTCTTGG	qRT-PCR analysis of HIF-1α mRNA level
rat-HIF-1α-mRNA-R	GTTTCTGCTGCCTTGTAT	
miR-1281-RT	GTGCAGGGTCCGAGGTCAGAGCCACCTGGGCAA TTTTTTTTTTTGGGAGA	Retro-transcription of mature miR-1281
miR-328-RT	GTGCAGGGTCCGAGGTCAGAGCCACCTGGGCAA TTTTTTTTTTTACGGAA	Retro-transcription of mature miR-328
snoRNA44-RT	GTGCAGGGTCCGAGGTCAGAGCCACCTGGGCAA TTTTTTTTTTTAGTCAG	Retro-transcription of snoRNA44
snoRNA202-RT	GTGCAGGGTCCGAGGTCAGAGCCACCTGGGCAA TTTTTTTTTTTCATCAG	Retro-transcription of snoRNA202
miR-1281-F	CCGGGTCGCCTCCTCCT	Forward primer for qRT-PCR analysis of miR-1281
miR-328-F	CACCCTGGCCCTCTCTGCCCT	Forward primer for qRT-PCR analysis of miR-328
snoRNA44-F	CATGAAGGTCTTAATTAGCTCTA	Forward primer for qRT-PCR analysis of snoRNA44
snoRNA202-F	GTACTTTTGAACCCTTTTCCAT	Forward primer for qRT-PCR analysis of snoRNA202
miRNA/snoRNA-R	CAGTGCAGGGTCCGAGGT	Universal reverse primer for qRT-PCR analysis of miRNA/snoRNA
CpG-F1	GGGGGGGGYGGGAGTTTTTAGTATTTGG	First round of PCR primer for CpG island
CpG-R1	CACCCTACRAACCCTCCTCCTCCTCC	
CpG-F1	GGGYGTGAGGGTT AGAGAGG	Second round of PCR primer for CpG island
CpG-R1	AATAACCRCACTAAACTCACCC	

Figure S1. MiR-1281 does not influence the expression of contractile maker proteins in PASMCs.

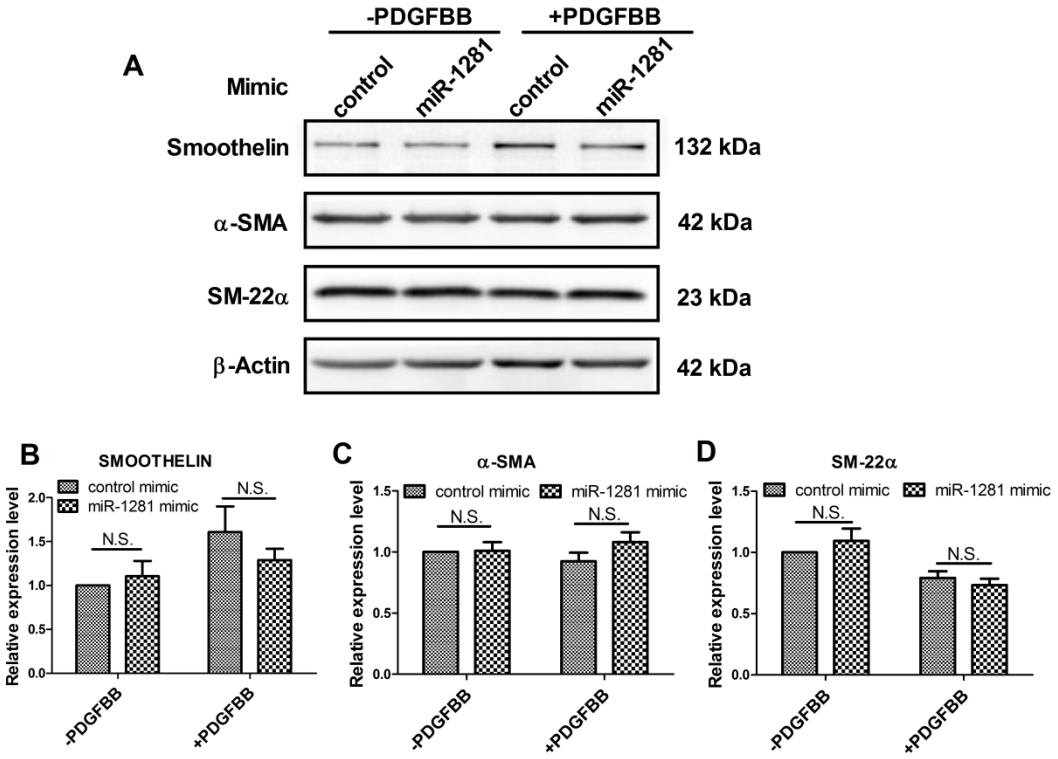

A) Representative figures of western blot assay on protein expression of Smoothelin,α -SMA and SM-22α in PASMCs transfected with either control mimic or miR-1281 mimic. Both culturing conditions without and with PDGFBB treatments were considered.β -Actin was used as loading control. Statistical analysis showing that the protein level of Smoothelin **B)**,α -SMA **C)** and SM-22α **D)** were not significantly altered by over-expression of miR-1281, under either culturing condition. N.S. indicates no significant difference.

Figure S2. PTPRD is a direct target of miR-1281 but its expression is not primarily regulated by miR-1281 in PDGFBB-treated PASMCs.

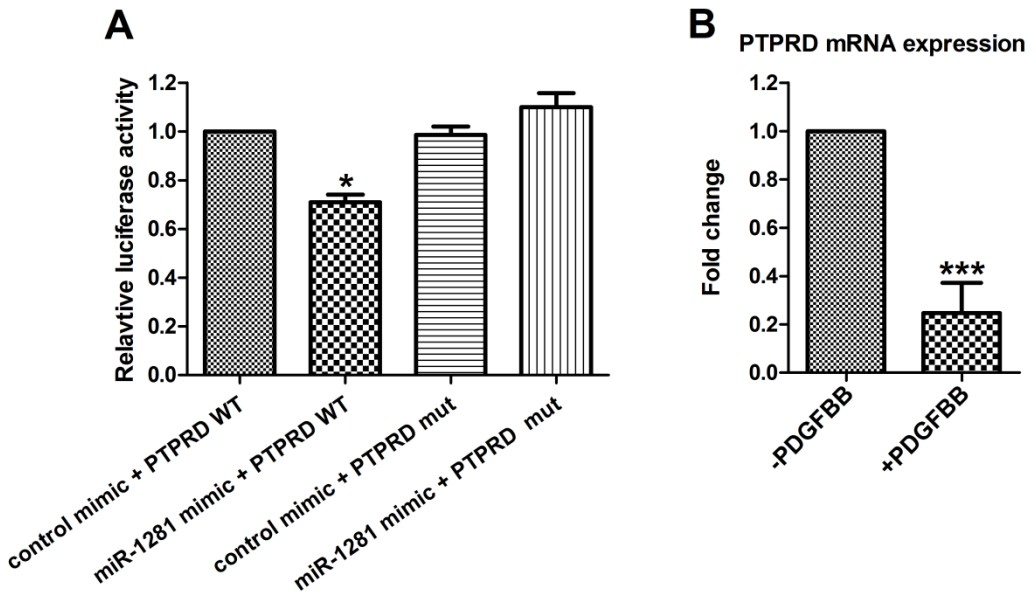

A) luciferase reporter assay demonstrating that PTPRD 3'UTR carries functional miR-1281 binding site, mutation of which abolished miR-1281 mimic inhibition of luciferase expression. However, **B)** qRT-PCR assay found that mRNA level of PTPRD significantly reduced in PDGFBB-treated PASMCs, suggesting its expression is not deregulated by reduced miR-1281 expression.

Figure S3. HDAC4 promotes PASMC proliferation and migration.

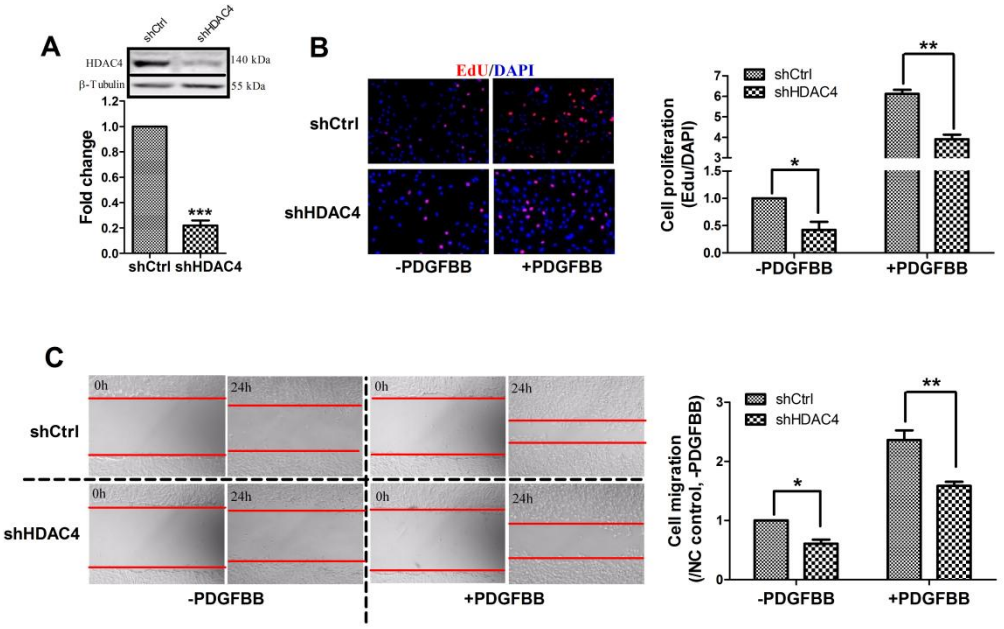

A) Western blotting analysis of silencing efficiency of shHDAC4 in PASMCs. –βTubulin was used as loading control. **B)** Representative figures of EdU assay and statistic analysis showing that shHDAC4 suppressed PASMC proliferation in the absence or presence of PDGFBB. **C)** Representative figures of wound-healing and statistic analysis showing that shHDAC4 suppressed PASMC migration in the absence or presence of PDGFBB.

Figure S4. Over-expression of miR-1281 does not significantly alter histone acetylation status of PASMCs.

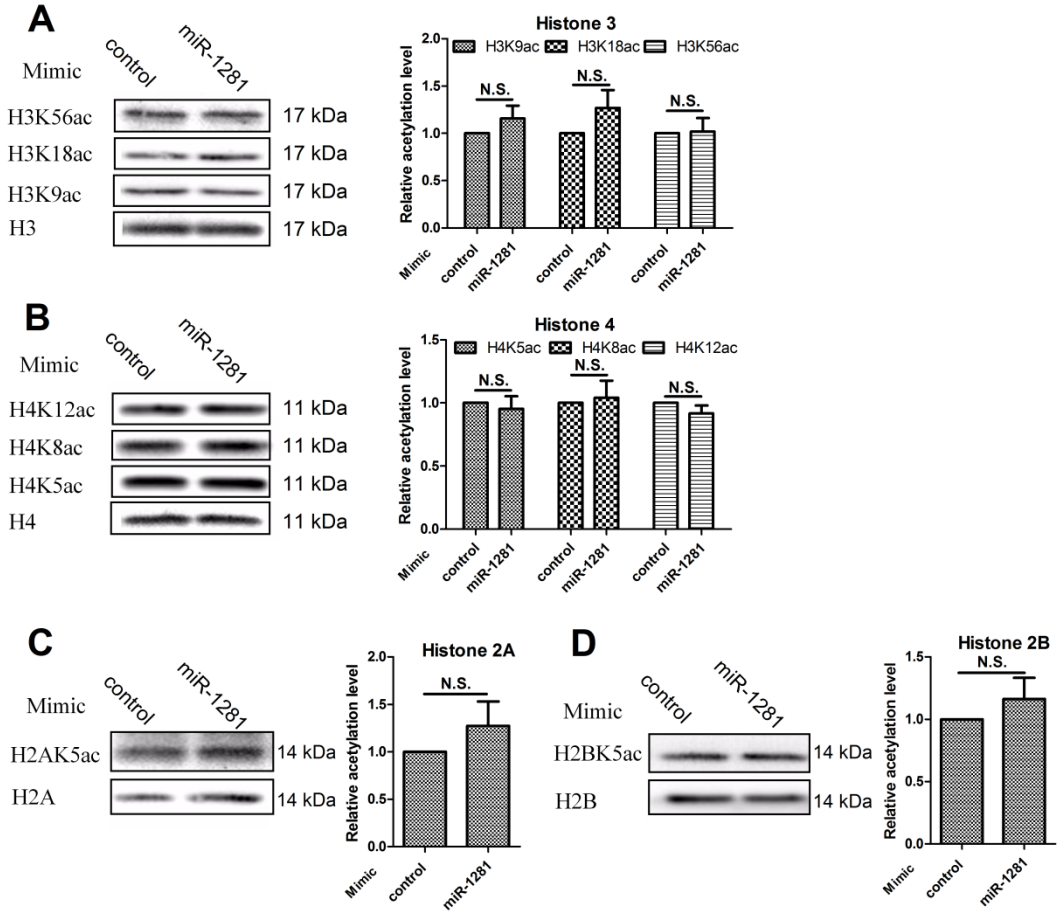

Western blot assay of acetylated Histone H3 **A)**, H4 **B)**, H2A **C)** and H2B **D)** were performed by examining respective acetylation sites (i.e. lysine residues as specified in each representative blotting figure, left panels). Corresponding total Histone was used as loading control. Statistic analysis found no significant difference of the acetylation status in miR-1281 mimic- or control mimic-transfected PASMCs. N.S. indicates no significant difference (right panels).

Figure S5. EGR1 does not influence the expression of miR-1281 in PDGFBB-treated PASMCs.

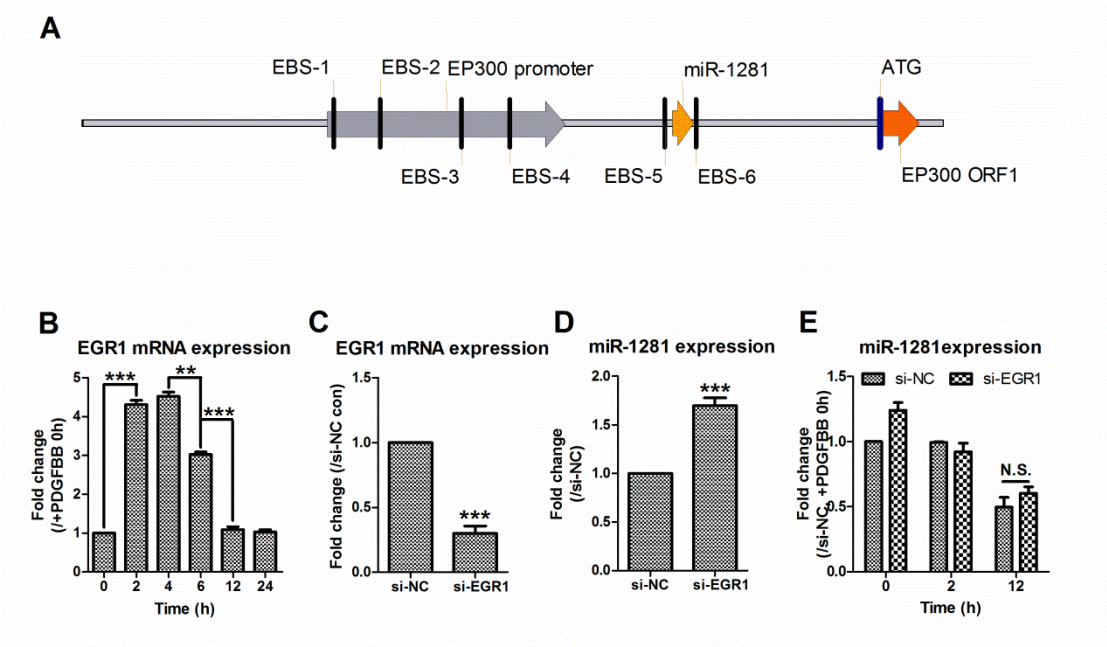

A) Illustration of EGR1 binding sites (EBS) identified in EP300 promoter and flanking regions of rat genome. **B)** Time-course assay of PDGFBB effect on EGR1 mRNA level in rat PASMCs. **C)** Transfection of si-EGR1 significantly inhibited EGR1 mRNA expression in PASMCs. **D)** This led to an up-regulation of miR-1281 expression; **E)** but effect of si-EGR1 did not influence the PDGFBB- repressed expression of miR-1281 at 12h.

Figure S6. PDGFBB induces DNA methylation of CpG island 5' upstream of MIR-1281/EP300 gene.

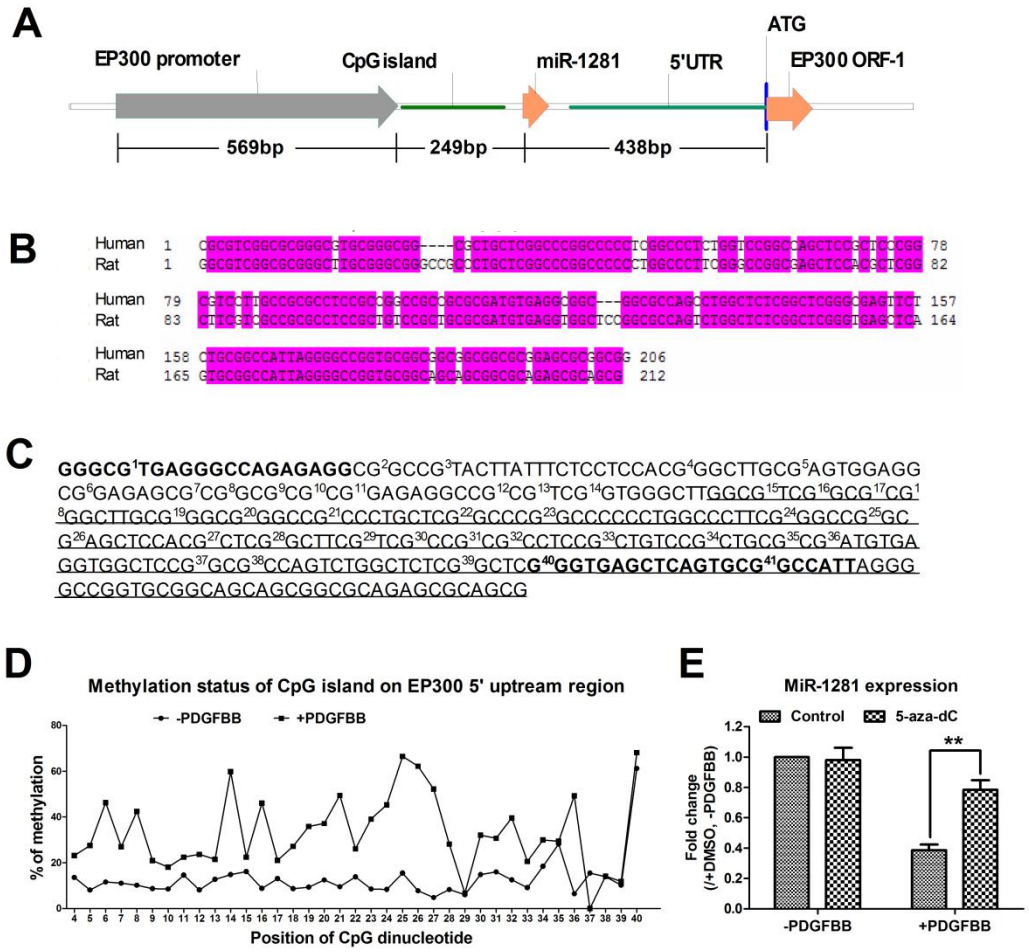

A) Illustration of location of predicted CpG island in the 5' upstream region of MIR-1281/EP300 gene. **B)** Sequence alignment of this CpG island between the human and rat genomes displayed high conservation. **C)** Detailed sequence information of bisulfite PCR amplified region. Bold black Sequence indicates the location where nested PCR primer annealing. CG dinucleotides are numbered for methylation analysis. Underlined Sequence indicates CpG island. **D)** Bisulfite sequencing showed enhanced DNA methylation at cytosine residues in CG dinucleotide sites of this CpG island. The line graph presents percentage of methylated cytosine in each CG dinucleotide in a sequential 5' to 3' order as numbered in C). **E)** Pre-treatment of 5-aza-dC treatment recovered PDGFBB repression of miR-1281 in PASMCs.

Figure S7. miR-1281/HDAC4 pathway influences the mRNA expression of HIF-1α in PASMCs.

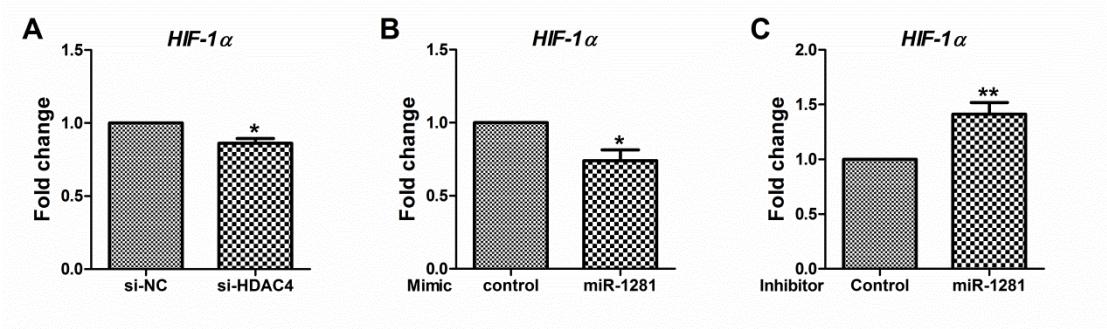

qRT-PCR analysis demonstrated that either inhibition of HDAC4 by si-HDAC4 **A),** or overexpression of miR-1281 by miR-1281 mimic **B),** decreased the mRNA level of HIF-1α in PASMCs; and inhibition of miR-1281 by miR-1281 inhibitor increased mRNA level of HIF-1α in PASMCs **C).**

Figure S8. PDGFBB-induced downregulation of miR-1281 is a specific phenomenon in PASMCs.

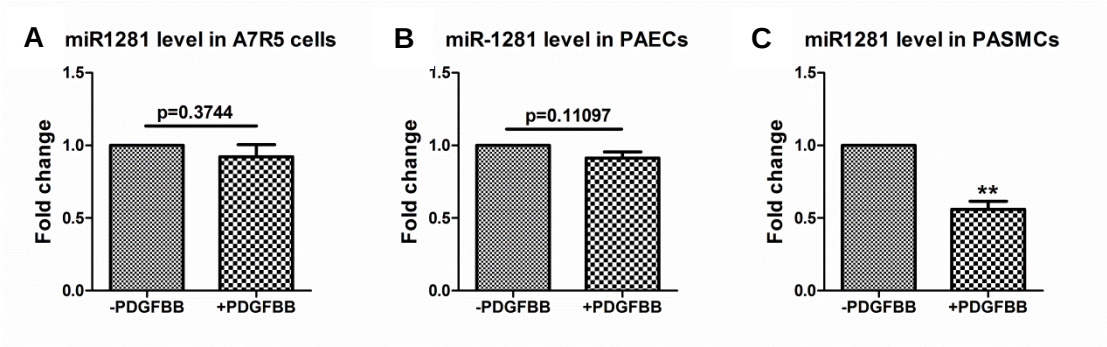

Aortic smooth muscle (A7R5) cell line, pulmonary arterial endothelial (PAEC) cells line, and PASMC cell lines were treated with PDGFBB (30ng/ml, 12h) respectively, qRT-PCR analysis found no change of miR-1281 level in RNA samples extracted from either PDGFBB-treated A7R5 **A**) or PAEC cells **B**), but significant reduction of miR-1281 level in PDGFBB-treated PASMC cells **C**). p values are presented to illustrate unsignificant differences.

Figure S9. Inhibition of PI3K kinase negatively influences the ERK phosphorylation.

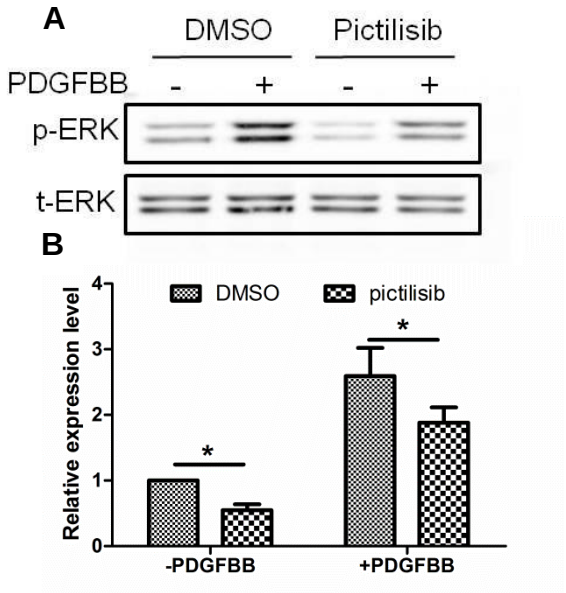

A) Representative figures of western blot assay on protein expression of phosphorylated ERK in PASMCs treated with PI3K inhibitor (Pictilisib) or DMSO (negative control). Both culturing conditions without and with PDGFBB treatments were considered. The total amount of ERK was used as loading control. **B)** Statistical analysis showing that PDGFBB treatment markedly induced ERK phosphorylation, while Pictilisib treatment decreased phosphorylation level of ERK in the absence of PDGFBB treatment, and attenuated the PDGFBB-induced ERK phosphorylation.

Figure S10. Expression of miR-1281 does not influence the expression of miR-328 in rat PASMCs.

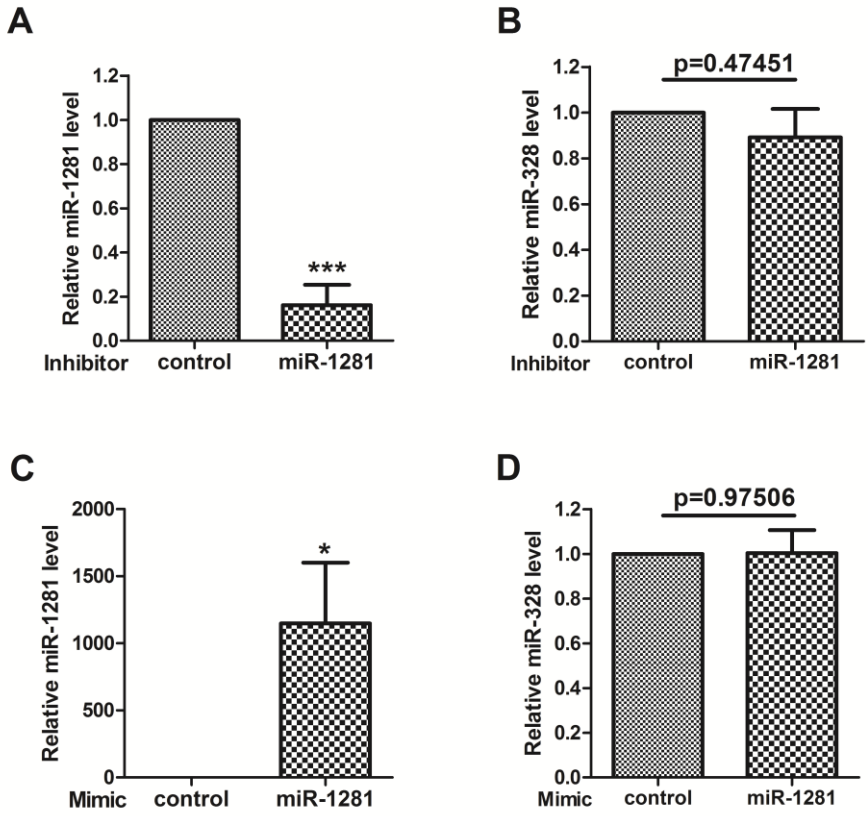

MiR-1281 inhibitor and mimic were transfected into rat PASMCs respectively. **A) & C)** qRT-PCR analysis of miR-1281 level verified the inhibition and overexpression efficacy. **B) & D)** qRT-PCR analysis of miR-328 level demonstrated that the change of miR-1281 expression does influence miR-328 level in PASMCs.

Figure S11. miR-1281 and miR-328 are independent miRNAs in terms of regulating human PASMC proliferation and migration.

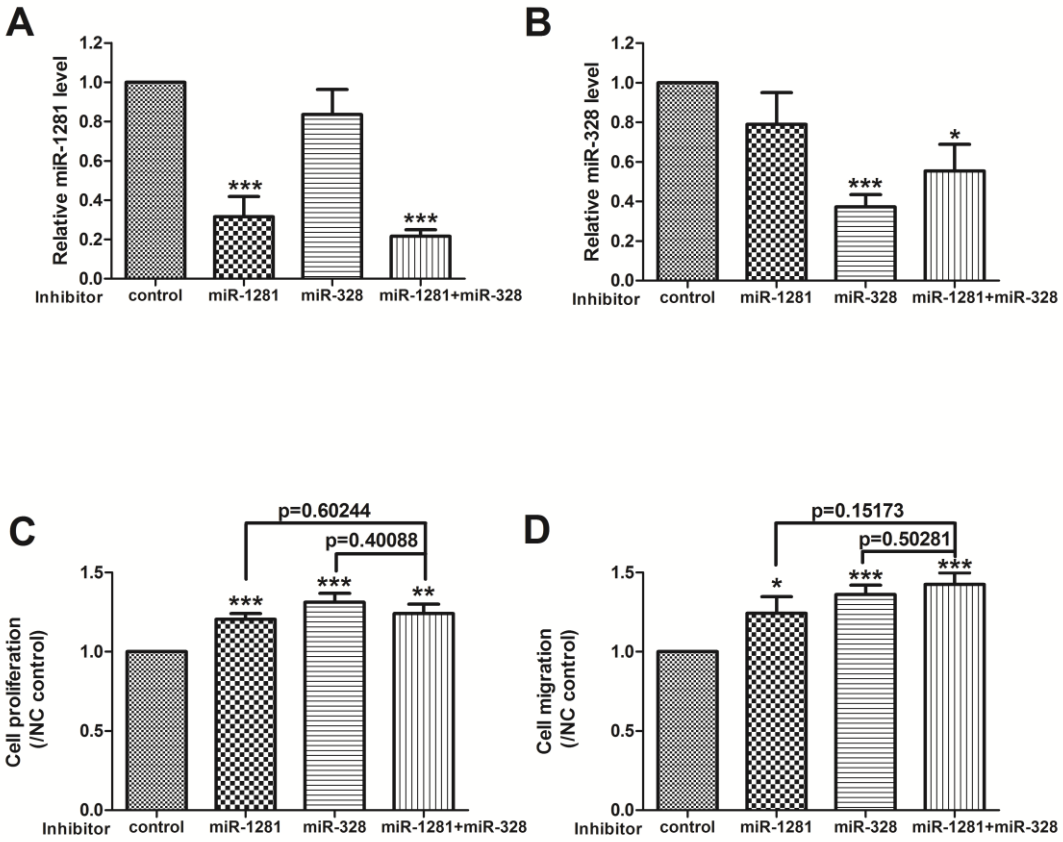

MiR-1281 inhibitor and miR-328 inhibitor were transfected individually or together into PASMCs for 48h. qRT-PCR analysis in RNA samples extracted from these PASMCs demonstrated that inhibition of miR-1281 would not influence the expression of miR-328 **A)**, and vice versa **B)**. Proliferation assay **C)** and migration assay **D)** performed on these cells demonstrated that simultaneous inhibition of both miR-1281 and miR-328 did not produce greater effect on PASMC proliferation or migration than individual inhibition. Each result presents the statistic analysis based on four independent batches of experiments.

Figure S12. Validation of MCT-induced PAH rat model.

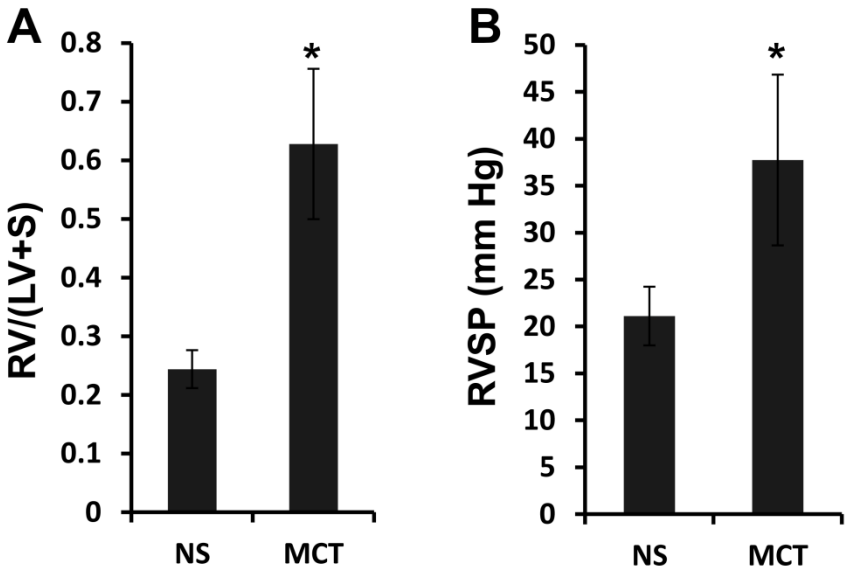

Rats injected with normal saline were used as control (NS). After 4 weeks, PAH development was assessed. Briefly, rats were anesthetized by an injection of pentobarbital sodium (30mg/kg), right jugular vein was surgically exposed and a 1.2-Fr pressure catheter connected to AP-621G (Nihon Kohden, Japan) was inserted into Right Ventricle (RV) through the incision in right jugular vein. Right Ventricular Systolic Pressure (RVSP) was recorded using MP150 system and AcqKnowledge software package (BIOPAC, Goleta, CA). To assess right ventricular hypertrophy, saline containing 5U/ml heparin was flushed into RV after death and the heart was removed. Then RV was separated from Left Ventricle (LV) and the ventricular Septum (S). Ratio of the weight of RV divided by that of LV plus S [RV/(LV+S)] was used to assess right ventricular hypertrophy. Both significantly higher RV/(LV+S) level (A) and higher RVSP level (B) of MCT-treated rat suggested an successful induction of PAH. (n=8)